Journal of Genetic Engineering and Biotechnology (2015) **13**, 93–99

HOSTED BY

ELSEVIER

Academy of Scientific Research & Technology and National Research Center, Egypt

Journal of Genetic Engineering and Biotechnology

www.elsevier.com/locate/jgeb

ARTICLE

Acorus calamus rhizome extract mediated biosynthesis of silver nanoparticles and their bactericidal activity against human pathogens

Chinnappan Sudhakar [a,1], Kandasamy Selvam [b,1], Muthusamy Govarthanan [a,c], Balakrishnan Senthilkumar [b], Arumugam Sengottaiyan [a], Murugesan Stalin [a], Thangasamy Selvankumar [a,*]

[a] *Department of Biotechnology, Mahendra Arts and Science College, Kalippatti, Namakkal 637501, Tamil Nadu, India*
[b] *Centre for Biotechnology, Muthayammal College of Arts and Science, Rasipuram, Namakkal 637 408, Tamil Nadu, India*
[c] *Division of Biotechnology, Advanced Institute of Environment and Bioscience, College of Environmental and Bioresource Sciences, Chonbuk National University, Iksan 570752, South Korea*

Received 29 June 2015; revised 9 October 2015; accepted 15 October 2015
Available online 4 November 2015

KEYWORDS

Biosynthesis;
Silver nanoparticles;
Rhizome;
Response surface methodology;
Bactericidal activity

Abstract Silver nanoparticle (AgNP) synthesis and characterization is an area of vast interest due to their broader application in the fields of science and technology and medicine. Plants are an attractive source for AgNP synthesis because of its ability to produce a wide range of secondary metabolites with strong reducing potentials. Thus, the present study describes the synthesis of AgNPs using aqueous rhizome extract of *Acorus calamus* (sweet flag). The AgNP formation was evaluated at different temperatures, incubation time and concentrations of $AgNO_3$ using Response surface methodology based Box–Behnken design (BBD). The synthesized AgNPs were characterized by UV–Visible spectroscopy, Fourier transform infra-red spectroscopy (FTIR), X-ray diffraction (XRD), and Scanning electron microscopy–energy-dispersive spectroscopy (SEM–EDS). The surface plasmon resonance found at 420 nm confirmed the formation of AgNPs. SEM images reveal that the particles are spherical in nature. The EDS analysis of the AgNPs, using an energy range of 2–4 keV, confirmed the presence of elemental silver without any contamination. The antibacterial activity of synthesized AgNPs was evaluated against the clinical isolates *Staphylococcus aureus* and *Escherichia coli* and it was found that bacterial growth was significantly inhibited in a dose dependent manner. The results suggest that the AgNPs from rhizome extract could be used as a potential antibacterial agent for commercial application.

* Corresponding author. Tel.: +91 9443470394.
E-mail address: t_selvankumar@yahoo.com (T. Selvankumar).
[1] The first two authors equally contributed this work.

Peer review under responsibility of National Research Center, Egypt.

http://dx.doi.org/10.1016/j.jgeb.2015.10.003
1687-157X © 2015 Production and hosting by Elsevier B.V. on behalf of Academy of Scientific Research & Technology.

1. Introduction

The field of nanotechnology is one of the most active areas of research in current material science. The synthesis and characterization of noble metal nanoparticles such as silver, gold and platinum is an emerging field of research due to their important applications in the fields of biotechnology, bioengineering, textile engineering, water treatment, metal-based consumer products and other areas, electronic, magnetic, optoelectronics, and information storage [31]. It has been reported that since ancient times silver is known to have antimicrobial activities [7,29] such as antifungal [5], antiviral [24], anti-angiogenesis [17], and silver nanoparticles (AgNPs) are of particular interest due to their peculiar properties and wide applications. Silver nanoparticles (AgNPs), as antibacterial agents, are now used extensively in the fields of medicine [6] and drug delivery [23].

Synthesis of AgNPs has been proposed as an emerging technology, and offers several applications to the scientific community. AgNPs have been synthesized by chemical [11,35], electrochemical [39], radiation [9], photochemical methods [4] and Langmuir–Blodgett [40,37] and biological techniques [28]. The latter has emerged as a green alternative, for it is environment-friendly, cost-effective, and easily scaled-up. It has great potential with natural reductants [34,2], such as plant extract [3], bacteria [16], fungus [14], panchakavya [12], and cow milk [21]. Plant extracts are more advantageous because using them eliminates the elaborate process of maintaining cell cultures and can be suitably scaled-up for large-scale production under nonaseptic environments, especially plants that secrete the functional molecules for the reaction, compatible with the green chemistry principles. There are some examples of synthesizing AgNPs using plants, such as *Helianthus tuberosus* [3], *Acacia leucophloea* [26], *Solanum indicum* [15], *Acalypha indica*, European Rowan (*Sorbus aucuparia*), and camphor laurel (*Cinnamomum camphora*) [30].

Antibacterial activity of medicinal plants becomes more recognized, an attempt is being made to establish the antibacterial activity of plant extracts used to synthesize AgNPs, and the combined effect of the metal and the plant extract. *Acorus calamus* is a natural plant belonging to the order *Acorales* and family *Acoraceae*. The genus name is *Acorus* and its species is called *A. calamus* [18]. This plant has a very long history of medicinal use in Chinese and Indian herbal traditions [13,25]. This plant was present in Indian markets nearly two thousand years ago [22] and it had been sold as a medicine in every Indian shop [36]. It was used for ailments such as dyspepsia [38], mouth and throat diseases, fevers, epilepsy, bronchitis, hysteria, tumors, rat bites, ear worms, toothaches, pains of the chest and kidneys, insomnia, melancholia, neurosis, loss of memory depression and mental disorders [20], asthma, diarrhoea, dysentery, flatulence [19,27].

The aim of the current study was (i) synthesis and optimization of AgNPs using rhizome extract of *A. calamus* (ii) Characterization of silver nanoparticles using UV–Vis spectroscopy, XRD, FT-IR, SEM–EDS and (iii) evaluation of the bactericidal activities against *Staphylococcus aureus*, *Bacillus cereus*, *Escherichia coli* and *Salmonella enterica* to check their biomedical importance.

2. Materials and methods

2.1. Materials

Silver nitrate of analytical grade was purchased from Merck. The glassware was washed in chromic acid and thoroughly washed with double distilled water and dried in hot air oven. The *A. calamus* rhizome was freshly collected from Yercaud, Salem, Tamil Nadu, India.

2.2. Preparation of the rhizome extract

Around 10 g of freshly collected *A. calamus* rhizome was ground well using mortar and pestle. 100 mL of deionized water was added into the slurry and filtered through a cheese cloth. The filtrate was again filtered through Whatman No. 1 filter paper (pore size 25 μm). The fresh filtrate was used for the present study.

2.3. Biosynthesis of AgNPs

Synthesis of silver nanoparticle methodology was developed according to Aravinthan et al. [3] with minor modifications. Briefly, 5 mL of rhizome extract was mixed with 50 mL of $AgNO_3$ (1–5 mM) solution and incubated at 30 °C for 48 h. The bio-reduction of $AgNO_3$ into AgNPs can be confirmed visually by the change in colour from colourless to reddish brown.

2.4. Statistical optimization of AgNP synthesis

Response surface methodology combined with BBD was established using Design Expert software (9.0.0.7 trial version). Three factors, namely, $AgNO_3$ concentration, incubation time, and temperature, were optimized for enhanced AgNP synthesis. Based on BBD, the factors were analysed at two levels: −1, for low level, and +1, for high level. A total of 17 runs were performed to optimize the process parameters, and experiments were performed according to the experimental design matrix. The results were evaluated by applying the coefficient of determination (R^2), analysis of variance (ANOVA) and response plots. Employing RSM, the most widely used second-order polynomial equation was developed to fit the experimental results and identify the relevant model terms.

$$Y = \beta_0 \Sigma \beta_i X_i + \Sigma \beta_i X_i \beta_{ij} + \Sigma X_i X_j \quad (1)$$

where, Y is the predicted response; β_0, β_i, and β_{ij} are constant regression coefficients of the model; and X_i and X_j represent independent variables. The experimental design chosen for the study was a Box–Behnken design that helps in investigating linear, quadratic and cross product effects of these factors, each varied at these levels and also includes three centre points for replication.

2.5. Characterization of AgNPs

Characterization of nanoparticles is important to understand and control nanoparticle synthesis and applications [1]. The bioreductive synthesis of AgNPs was monitored using a Shimadzu UV-2450 PC scanning double beam UV–Vis

spectrophotometer. The UV–Vis spectra were recorded between 200 and 600 nm as a function of temperature for the bioreductive property of aqueous *A. calamus* rhizome extract. The increase in 430 nm centred strong resonance bands was noted [3]. XRD was recorded in the 2θ range of 30–80° using XRD6000 (Shimadzu) of Cu Ka radiation, the energy of which was 8.04 keV and wavelength was 1.54 Å. The applied voltage was 40 kV and current was 25 mA. The crystallite size was estimated using the Scherer equation. The presence of functional groups in *A. calamus* rhizome extract and synthesized AgNPs was identified by Shimadzu-8400 FTIR Spectrometer using KBr pellet technique. Scanning electron microscope–energy-dispersive spectra (SEM–EDS) analysis was carried out using Jeol JSM 6390 model. Thin films of the sample were prepared on a carbon-coated copper grid by just dropping a very small amount of the sample on the grid, extra solution was removed using a blotting paper and then the film on the SEM grid was allowed to dry.

2.5.1. Evaluation of the bactericidal activity

The bactericidal activity of the AgNPs was evaluated against the clinical isolates *S. aureus*, *B. cereus* (Gram-positive) and *E. coli*, *S. enterica* (Gram-negative) obtained from Government Mohan Kumaramangalam medical College and Hospital, Salem, Tamil Nadu, India. The bactericidal activity was carried out with 24 h active cultures by employing the disc diffusion method [9]. About 150 CFU/mL of inoculums was swabbed onto Muller Hinton agar (MHA) plates uniformly and allowed to dry in a sterile environment. Sterile disc of 6 mm (HIMEDIA) was loaded with 30 µl of test solution (AgNPs 5 and 10 µg/mL). Ampicillin (10 µg/mL) was used as positive control. The plates were incubated at 26 °C for 2 days to measure the zone of inhibition. The mean was calculated by performing the experiments in triplicates.

3. Results and discussion

The synthesis of AgNPs was initially observed by the colour change from light yellow to dark brown. The colour change is due to the excitation of surface plasmon resonance vibrations in AgNPs. Similar results were observed in various plants studied by Aravinthan et al. [3]. Characteristic absorption peaks of AgNPs can be seen at around 420 nm. Fig. 1 shows the UV–Visible spectra of synthesized AgNPs and rhizome extract.

The BBD was applied to identify the optimal conditions for the enhanced AgNP synthesis. The experimental design is presented in Table 1. ANOVA of the quadratic regression model (Table 2) exhibits that it was a highly significant model, as was evident from Fisher's *F*-test with a very low probability value (*F value* = 107.41). Values of 'Prob > *F*' (0.0001) indicate that the term of the model was significant. The Model *F*-value of 107.41 implies that the model was significant. There was only a 0.01% chance that a model F-value could occur due to noise. The predicted R^2 (0.5649) and adjusted R^2 (0.7421) values for AgNP synthesis were in reasonable agreement with the value of R^2 (0.9200), which is closer to 1.0, indicating the better fitness of the model in the experimental data. As a model for rhizome mediated synthesis of AgNPs, three different tests, namely, sequential model sum of squares, lack of fit tests and model summary statistics were carried out in the present study.

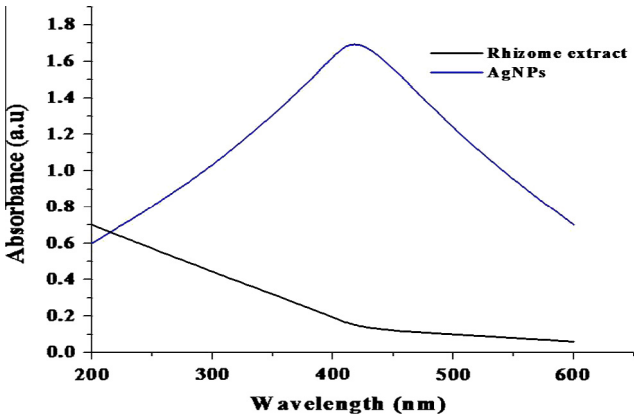

Figure 1 UV–Visible spectrum of biosynthesized AgNPs and rhizome extract.

Table 1 Box–Behnken design for the variables and the experimentally observed responses.

Run	$AgNO_3$ (mM)	Time (h)	Temperature (°C)	Absorbance at 420 nm
1	2	48	40	3
2	2	30	30	2.7
3	1	48	30	4
4	2	12	40	2
5	2	12	20	2
6	3	12	30	1.8
7	1	30	40	3.5
8	1	30	20	3.1
9	2	30	30	2.7
10	2	30	30	2.7
11	2	30	30	2.7
12	3	48	30	2
13	1	12	30	2.8
14	2	30	30	2.7
15	3	30	40	1.8
16	2	48	20	2.2
17	3	30	20	1.2

The contour plot graphical representations were generated (Fig. 2). The results demonstrate that there was a significant relation between $AgNO_3$ concentration, incubation time, and temperature for AgNP synthesis. Fig. 2(a) shows 1 mM solution, AgNPs have shown absorbance maxima at 420 nm, broadening of the peak indicates that the nanoparticles are polydispersed, 2 mM solution has peak at 420 nm corresponding to AgNPs which may be attributed to the presence of bioactive components as capping agents on the surface of nanoparticles, 3 mM solution has at 435 nm. The spectrum shows the red shift with an increasing molar concentration of silver nitrate. It indicates the increase of mean diameter of the AgNPs as the concentration increases [10]. The silver nitrate concentration 3 mM indicates a faster rate of bioreduction with increased concentration of precursor salt. The increase in silver nitrate concentration of 5 mM and above

Table 2 Analysis of variance (ANOVA) for the response surface quadratic model.

Source	Sum of squares	Df	Mean squares	*F* value	*p*-value Prob > *F*
Model	7.60	9	0.84	107.41	< 0.0001
A-$AgNO_3$	5.44	1	5.44	693.00	< 0.0001
B-time	0.85	1	0.85	107.55	< 0.0001
C-temperature	0.41	1	0.41	51.55	0.0002
AB	0.25	1	0.25	31.82	0.0008
AC	0.010	1	0.010	1.27	0.2964
BC	0.16	1	0.16	20.36	0.0028
A^2	2.632E-003	1	2.632E-003	0.33	0.5809
B^2	0.024	1	0.024	3.01	0.1261
C^2	0.44	1	0.44	56.60	0.0001
Residual	0.055	7	7.857E-003		
Lack of fit	0.055	3	0.018		
Pure error	0.000	4	0.000		
Cor. total	7.65	16			

leads to peaks with lower intensity which can be accounted for by the formation of agglomerated nanoparticles and their settling. The presence of very large particles was the cause of faster settling of particles [32]. Fig. 2(b) shows the UV–Vis absorption spectra of reaction mixtures studied at different levels of incubation time (12–48 h). Fig. 2(c) shows the UV–Vis absorption spectra of reaction mixtures studied at different levels of temperature (20–40 °C). From the absorption spectra, it is noted that Ag surface Plasmon resonance band occurs at about 420 nm and the intensity of absorption increases steadily as a function of incubation time. The optimum levels of the variables were obtained by using BBD. The model predicted a maximum AgNP synthesis appearing in 1 mM $AgNO_3$ concentration, 48 h and 30 °C. Predicted model was validated and experiments were conducted using these optimal conditions. The predicted model values were in good agreement with the values measured in these experiments, thus mitigating the validity of the response model and the necessity for optimal conditions.

The coefficients of the regression equation were calculated and the following regression equation was obtained.

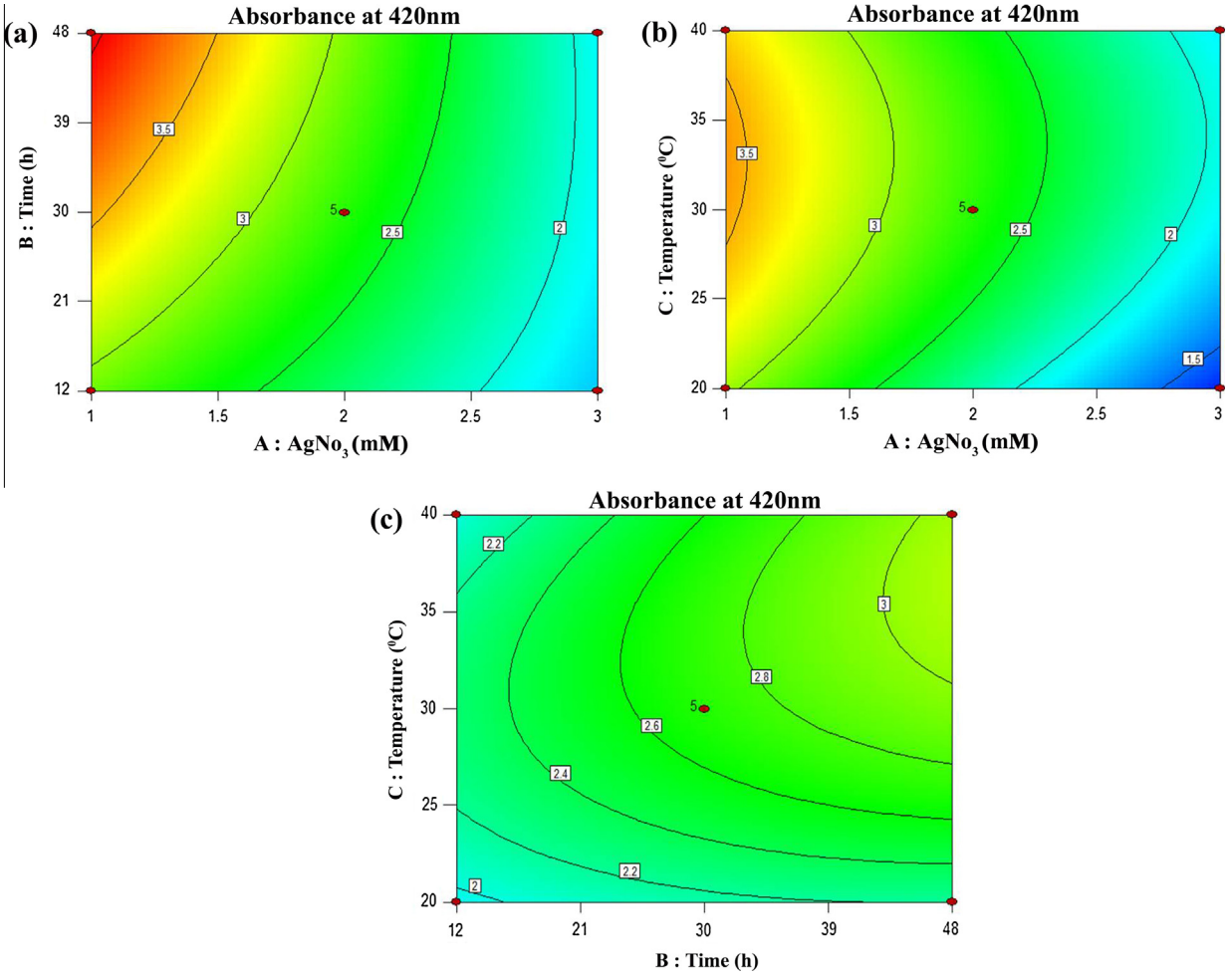

Figure 2 Contour plots of the combined effects of two variables on *A. calamus* rhizome mediated synthesis of AgNPs. (a) $AgNO_3$ and time as variables at fixed temperature, (b) $AgNO_3$ and temperature as variables at a fixed incubation time and (c) incubation time and temperature as variables at a fixed $AgNO_3$.

$$Y(\text{Absorbance at } 420\text{ nm}) = +2.70 - 0.82A + 0.33B + 0.23C - 0.25AB + 0.050AC + 0.20BC + 0.025A^2 - 0.075B^2 - 0.33C^2 \quad (2)$$

where, Y stands for AgNP synthesis (Absorbance at 420 nm), A is $AgNO_3$ concentration, B is incubation time, C is temperature respectively. A high degree of similarity of experimental values was observed, thus reflecting the precision and applicability of RSM to optimize the process for AgNP synthesis.

The sample of AgNPs could be also characterized by X-ray diffraction analysis of dry powders. The diffracted intensities were recorded from 10° to 90° at 2θ angles (Fig. 3). Four different and important characteristic peaks were observed at the 2 h of, 28.11°, 32.56°, and 46.54°, that correspond to (111), (200), and (220), planes, respectively. All the peaks in XRD pattern can be readily indexed to a face-centred cubic structure of silver as per available literature (JCPDS, File No. 893722). The average crystal size of the silver crystallites was calculated from the FWHMs of the diffraction peaks, using the Scherrer equation. It was found that the average size from XRD data and using the Debye–Scherrer equation was approximately 35 nm. The results are in agreement with those of several studies that reported the cubic nature of biologically synthesized AgNPs [3,33].

The FTIR spectra of *A. calamus* rhizome extract and biosynthesized AgNPs, shown in Fig. 4, indicate the presence of amino, carboxylic, hydroxyl and carbonyl groups. Display of strong broad O–H stretch carboxylic bands in the region 3412.08 cm^{-1} and carboxylic stretching bands in the region 1564 cm^{-1} was observed. The peaks appearing in the region 1645 cm^{-1} are attributed to the stretching vibration of the NH group that is characteristic of proteins shifted from 1384 cm^{-1} after the synthesis of Ag-NPs. The secondary structure was not affected during reaction with Ag + Ions or after binding with Ag nanoparticles. These results confirm the presence of possible proteins.

The SEM analysis was used to determine the structure of the reaction products that were formed. The SEM image showed individual silver particles as well as a number of aggregates, SEM images of SNPs derived from the rhizome extracts

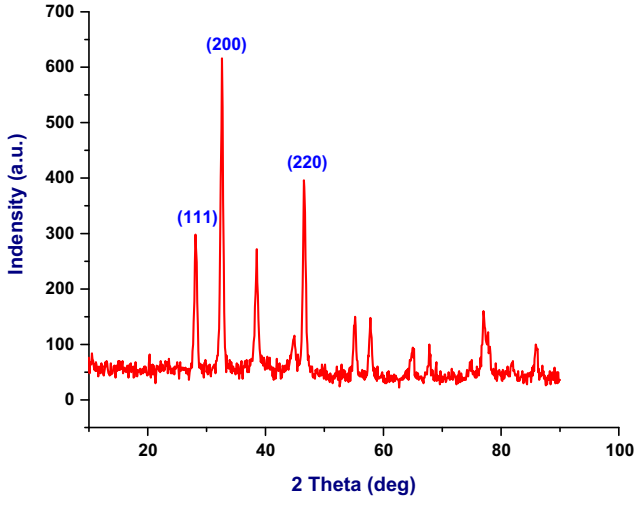

Figure 3 FT-IR spectra of AgNPs synthesized from *A. calamus* rhizome extract.

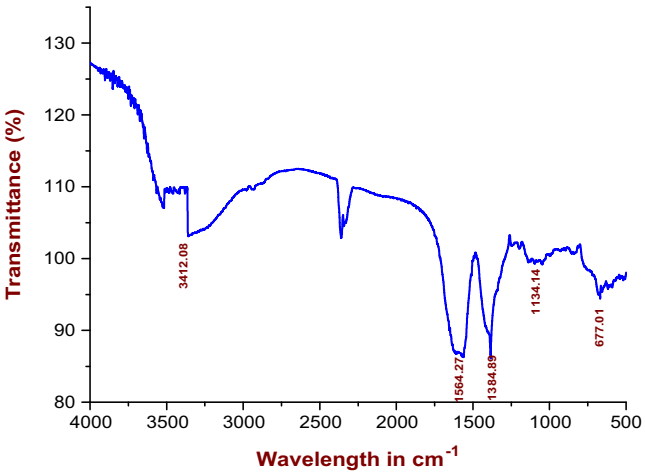

Figure 4 XRD pattern of AgNPs synthesized using *A. calamus* rhizome extract.

of *A. calamus* showed particles to be in spherical shape with size ranging from 20 to 35 nm (Fig. 5). The morphology of the SNPs was predominantly spherical and they appear to be monodispersed (a and b). Further, analysis of the silver particles by energy dispersive spectroscopy confirmed the presence of the signal characteristic of silver (c).

The bactericidal activity of the biosynthesized AgNPs against different human pathogens is shown in Fig. 6. It is apparent that the AgNPs showed inhibition zones against almost all the test organisms. Maximum zone of inhibition was found in 10 µg/mL of AgNP concentration against gram positive *S. aureus* (15 mm), and minimum zone of inhibition was obtained against *S. enterica* (8 mm) compared with rhizome extract. The AgNPs synthesized via green route are highly toxic towards bacterial strains. Silver ions have been demonstrated to interact with the protein and possibly phospholipids associated with the proton pump of bacterial membranes. This results in a collapse of membrane proton gradient causing a disruption of many of the mechanisms of cellular metabolism and hence cell death [8].

4. Conclusions

Biosynthesis promises an eco-friendly and non-toxic route to synthesize AgNPs. *A. calamus* rhizome was proved to be one of the potential sources to produce stable and well-defined nanoscale silver particles. UV–Visible spectroscopy showed peaks in the range 420 nm confirming the formation of AgNPs. Response surface methodology based Box–Behnken design (BBD) was used to optimize the variables such as $AgNO_3$ concentration, incubation time, temperature for AgNP synthesis. The FTIR studies indicate the capping of certain amide-containing compounds on the synthesized AgNPs. SEM–EDS analysis showed that the biosynthesized AgNPs are spherical in nature and elemental silver is present. The synthesized AgNPs exhibited a strong antibacterial activity against both Gram-negative and Gram-positive bacteria. The data obtained in this study indicate that it would be important to know the mechanism of action of the biosynthesized nanoparticles before their use in nanomedicine applications.

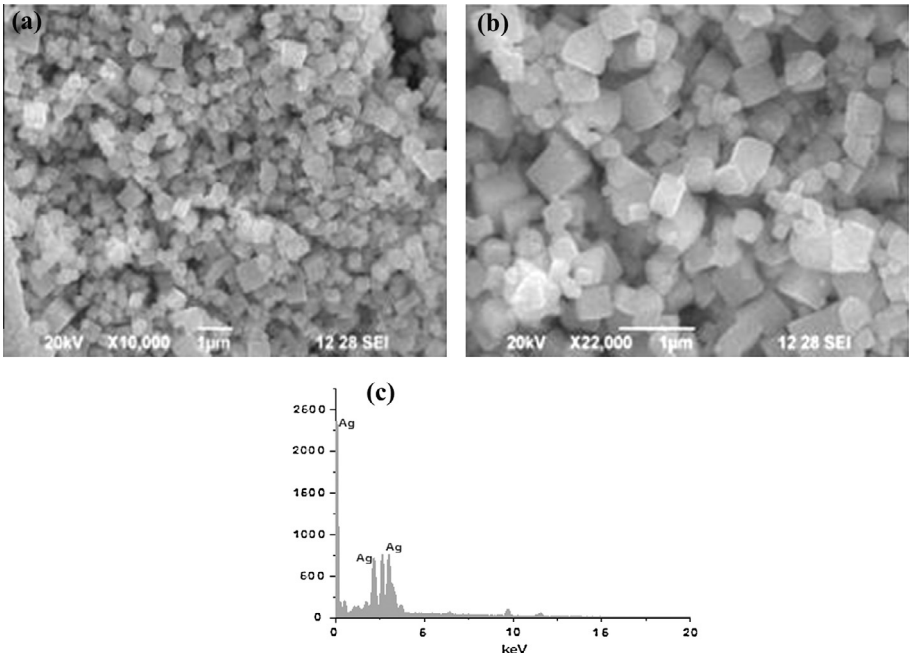

Figure 5 (a and b) SEM images of AgNPs show spherical shape (c) EDS spectrum of AgNPs which confirmed the presence of elemental silver.

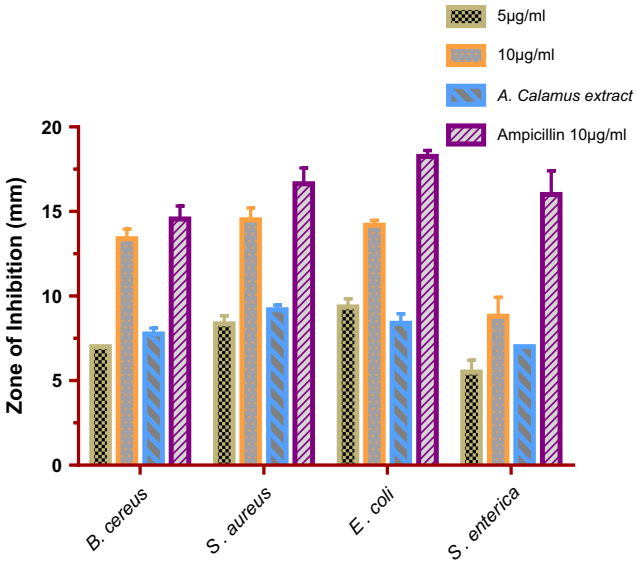

Figure 6 Antibacterial activity of rhizome extract and AgNPs. Error bars indicate standard deviation of means, where absent, bars fall within symbols.

References

[1] A. Al-Warthan, M.M. Kholoud, A. El-Nour, A. Eftaiha, R.A. A. Ammar, Arabian J. Chem. 3 (2010) 135–140.
[2] J.J. Antony, P. Sivalingam, D. Siva, Colloids Surf. B 88 (1) (2011) 134–140.
[3] A. Aravinthan, M. Govarthanan, K. Selvam, L. Praburaman, T. Selvankumar, R. Balamurugan, S. Kamala-Kannan, Jong-Hoon Kim, Int. J. Nanomed. 10 (2015) 1977–1983.
[4] A. Callegari, D. Tonti, M. Chergui, Nano Lett. 3 (2003) 1565–1568.
[5] G. Chladek, A. Mertas, I. Barszczewska-Rybarek, Int. J. Mol. Sci. 12 (7) (2011) 4735–4744.
[6] M.A. Dar, A. Ingle, M. Rai, Nanomedicine 9 (1) (2013) 105–110.
[7] L.S. Devi, S.R. Joshi, Mycobiology 40 (1) (2012) 27–34.
[8] P. Dibrov, J. Dzoiba, K.K. Gosink, C.C. Hase, Antimicrob. Agents Chemother. 46 (2002) 2668–2770.
[9] N.M. Dimitrijevic, D.M. Bartels, C.D. Jonah, K. Takahashi, T. Rajh, Phys. Chem. B. 105 (2001) 954–959.
[10] A.M. Fayaz, K. Balaji, P.T. Kalaichelvan, R. Venkatesan, Colloids Surf. B 74 (2009) 123–126.
[11] M.S. Ghassan, H.M. Wasnaa, R.M. Thorria, A.A.A. Ahmed, A.K.H. Abdul, B.M. Abu, Asian Pac. J. Trop. Biomed. 3 (1) (2013) 58–63.
[12] M. Govarthanan, T. Selvankumar, K. Manoharan, Int. J. Nanomed. 9 (2014) 1593–1599.
[13] M.R. Howes, P.J. Houghton, Pharmacol. Biochem. Behav. 75 (2003) 513–527.
[14] A. Ingle, A. Gade, S. Pierrat, C. Sonnichsen, M. Rai, Curr. Nanosci. 4 (2) (2008) 141–144.
[15] A. Sengottaiyan, R. Mythili, T. Selvankumar, A. Aravinthan, S. Kamala-Kannan, K. Manoharan, P. Thiyagarajan, M. Govarthanan, J.H. Kim, Res. Chem. Intermed. (2015), http://dx.doi.org/10.1007/s11164-015-2199-7.
[16] K. Kalimuthu, R. Suresh Babu, D. Venkataraman, M. Bilal, S. Gurunathan, Colloids Surf. B 65 (1) (2008) 150–153.
[17] K. Kang, D.H. Lim, I.H. Choi, Toxicol. Lett. 205 (3) (2011) 227–234.
[18] R.V. Lansdown, "Acorus calamus". IUCN Red List of Threatened Species. International Union for Conservation of Nature, 2014. Version 2014.2.
[19] H. Kim, T.H. Han, S.G. Lee, J. Ethnopharmacol. 122 (2009) 149–156.
[20] K.R. Kirtikar, B.D. Basu, Indian Medicinal Plants, vol. IV. M/S. Bishen Singh Ma-hendra Pal Singh, New Connaught Place, Debra Dun, India, 1975.
[21] K.J. Lee, S.H. Park, M. Govarthanan, Mater. Lett. 205 (3) (2013) 128–131.

[22] J.U. Lloyd, Origin and History of all the Pharmacopeial Vegetable Drugs, Caxton Press, Cincin-nati, 1929.
[23] H. Meng, M. Liong, T. Xia, ACS Nano 4 (8) (2010) 4539–4550.
[24] A. Mohammed, Z. Fayaz, M. Ao, Girilal, Int. J. Nanomed. 7 (2012) 5007–5018.
[25] Motley J. Timothy, Econ. Bot. 48 (4) (1994) 397–412.
[26] K. Murugan, B. Senthilkumar, D. Senbagam, Saleh Al-Sohaibani, Int. J. Nanomed. 9 (2014) 2431–2438.
[27] S. Nandakumar, S. Menon, S. Shailajan, Biomed. Chromatogr. 27 (2013) 318–326.
[28] R.R. Naik, S.J. Stringer, G. Agarwal, S. Jones, M.O. Stone, Nat. Mater. 1 (2002) 169–172.
[29] S. Pal, Y.K. Tak, J.M. Song, Appl. Environ. 73 (2007) 1712–1720.
[30] P. Prakash, P. Gnanaprakasam, R. Emmanuel, S. Arokiyaraj, M. Saravanan, Colloids Surf. B 108 (2013) 255–259.
[31] Z.Z. Rafiuddin, Colloids Surf. B 108 (2013) 90–94.
[32] A.A. Safekordi, H. Attar, H.R. Ghorbani, S. Sorkhabadi, M. Rezayat, Asian J. Chem. 23 (2011) 5111–5118.
[33] A. Sasikala, M. Linga Rao, N. Savithramma, Appl. Nanosci. 5 (2015) 827–835.
[34] P. Sivalingam, J.J. Antony, D. Siva, S. Achiraman, K. Anbarasu, Colloids Surf. B 98 (2012) 12–17.
[35] Y. Sun, Y. Yin, B.T. Mayers, T. Herricks, Y. Xia, Chem. Mater. 14 (2002) 4736–4745.
[36] T. Sylvan, F. Runkel, Bull, Alvin, Wildflowers of Iowa Woodlands, University of Iowa Press, Iowa City, Iowa, 2011, pp. 119.
[37] A. Swami, P.R. Selvakannan, R. Pasricha, M. Sastry, J. Phys. Chem. B 108 (2004) 19269.
[38] R.C. Wren, Potter's new Cyclopaedia of Botanical Drugs and Preparations, Sir Isaac Pitman and Sons Ltd., London, 1956.
[39] B. Yin, H. Ma, S. Wang, S. Chen, J. Phys. Chem. B 107 (2003) 8898–8904.
[40] L. Zhang, Y.H. Shen, A.J. Xie, S.K. Li, B.K. Jin, Q.F. Zhang, J. Phys. Chem. B. 110 (2006) 6615–6620.